Proceedings of the 1998 IEEE/RSJ
Intl. Conference on Intelligent Robots and Systems
Victoria, B.C., Canada • October 1998

Trajectory Generation using Time Scaled Artificial Potential Field

Yoshiyuki Tanaka† Toshio Tsuji† Makoto Kaneko† Pietro G. Morasso††

†Industrial and Systems Engineering, Hiroshima University
Kagamiyama, Higashi-Hiroshima 739-8527, JAPAN
††Department of Informatics, System and Telecommunications, University of Genova
Via Opera Pia 13, 16145 Genova, ITALY

Abstract

A new trajectory generation method for the dynamic control of robots is proposed in this paper. The proposed method is developed by introducing the combination of a time scale transformation with a time base generator into the Artificial Potential Field Approach (APFA). *This method can actively control the dynamic behavior of the robot without any change of the form of the designed controller itself. Effectiveness of the proposed method is verified through computer simulations with an omnidirectional mobile robot.*

1 Introduction

In the Artificial Potential Field Approach (APFA) [1]–[4], the goal is represented by an artificial attractive potential field and the obstacles by corresponding repulsive fields, so that the trajectory to the target can be associated with the unique flow-line of the gradient field originating at the initial position and can be generated via a flow-line tracking process. This method is often used for the trajectory generation problem of vehicles and manipulators because of its simplicity and lower computation than other methods that are based on global information about the task space. However, little attention has been paid to the control of the dynamic behavior of the generated trajectories such as movement time from the initial position to the goal and velocity profile of the generated trajectory.

For the disadvantage of the artificial potential field approach mentioned above, H. Hashimoto et al. [4] proposed a method using an electrostatic potential field and a sliding mode for a manipulator that can regulate the movement time but not the dynamic behavior of a robot. Recently, T. Tsuji et al. [5] [6] proposed a method introducing the Time Base Generator (TBG) into the APFA which can regulate the movement time and also the velocity profile of the robot, but can not be applied to the dynamic control.

Generally, it is harder to develop the dynamic control of the robot than the kinematic control because of the existence of a drift part in the dynamic system. In fact, without respect to holonomy or non-holonomy of the system, most previous studies have dealt with the kinematic model for the trajectory generation problem.

On the other hand, M. Sampei and K. Furuta [7] showed that the stability of a system is preserved for any time scale transformation as long as the defined new time never goes backward against the actual time. Then, they proposed the time scale transformation for a linearized non-linear system and applied it to the trajectory path following problem of a non-holonomic mobile robot [8].

In this paper, we first show that the TBG method [5] [6] developed for the kinematic model of the robot is equivalent to the time scale transformation with the time scale function composed by the TBG. Then a new trajectory generation method is proposed as a consequence of reformulating the TBG method in view of the time-scaling which can be applied to the dynamic model of the robot. The proposed method can control the dynamic behavior of the robot without any change of the form of the designed controller itself.

This paper is organized as follows: Section **2** points out the general problems of the APFA. Then, the new trajectory generation method based on the APFA is explained in detail in Section **3**. Finally, the propose method will be applied to the dynamic model of an omnidirectional mobile robot and the effectiveness will be shown from computer simulations in Section **4**.

2 Artificial Potential Field Approach

We consider the following dynamic linear system with a drift part:

$$\frac{d}{dt}\boldsymbol{X} = \boldsymbol{P}\boldsymbol{X} + \boldsymbol{Q}\boldsymbol{F}_X, \tag{1}$$

where

$$\boldsymbol{P} = \begin{pmatrix} \boldsymbol{0}_{n+n} & \boldsymbol{I}_{n+n} \\ \boldsymbol{0}_{n+n} & \boldsymbol{0}_{n+n} \end{pmatrix}, \quad \boldsymbol{Q} = \begin{pmatrix} \boldsymbol{0}_{n+n} \\ \boldsymbol{I}_{n+n} \end{pmatrix},$$

$\boldsymbol{X} = (\boldsymbol{x}^T, \dot{\boldsymbol{x}}^T)^T \in \Re^{2n}$ is the state variable vector, $\boldsymbol{F}_X \in \Re^n$ is the input vector, $\boldsymbol{0}_{n+n} \in \Re^{n\times n}$ is the zero matrix and $\boldsymbol{I}_{n+n} \in \Re^{n\times n}$ is the unit matrix.

0-7803-4465-0/98 $10.00 © 1998 IEEE

In order to clarify our purpose in this paper, we attempt to design the feedback control law F_X using the conventional APFA to stabilize the system (1) asymptotically. In this case, the potential function with quadratic form V_X can be defined as

$$V_X = \frac{1}{2} X^T K_0 X, \tag{2}$$

where $K_0 = \text{diag.}\ (k_1, k_2, \cdots, k_{2n})$ under $k_i > 0$ $(i = 1, \cdots, 2n)$. When we design the feedback control law F_X based on the potential function V_X as

$$F_X = -K_1 X\,, \tag{3}$$

the time derivative of the potential function $\dot{V}_X$ yields

$$\dot{V}_X = -X^T K_2 X \leq 0\,, \tag{4}$$

where

$$K_1 = \left(\begin{array}{cccc|c} \frac{k_1}{k_{n+1}} & 0 & \cdots & 0 & \\ 0 & \frac{k_2}{k_{n+2}} & \cdots & 0 & \\ \vdots & \vdots & \ddots & \vdots & I_{n+n} \\ 0 & 0 & \cdots & \frac{k_n}{k_{2n}} & \end{array} \right),$$

$$K_2 = \text{diag.}(0, 0, \cdots, 0, k_n, k_{n+1}, \cdots, k_{2n})\,.$$

Hence, V_X is controlled to the equilibrium point $X = \mathbf{0}$ by means of the feedback control law F_X given in (3). Moreover, substituting (3) into (1), we can derive the following linear damped system:

$$\ddot{x} + \dot{x} + K_3 x = \mathbf{0}\,, \tag{5}$$

where

$$K_3 = \text{diag.}(\frac{k_1}{k_{n+1}}, \frac{k_2}{k_{n+2}}, \cdots, \frac{k_n}{k_{2n}})\,.$$

Obviously, the system given in (1) is asymptotically stable under the designed feedback controller F_X. Following the above discussion, we can conclude that it is impossible to regulate the convergence time and the dynamic behavior of the vehicle as hoped [6].

3 Time Scaled APFA

Generally, the stability and dynamic property of systems have no change in any time scale that is a strictly monotone increasing function with respect to the actual time [7]. This indicates that we can design the feedback control law to converge the original system (1) to the equilibrium point at finite time t_f, if the asymptotic stabilizer for the system in the new time scale where infinite time corresponds to t_f in the actual time is found.

In this section, we present a detail of the proposed method based on the APFA combined with the time scale transformation.

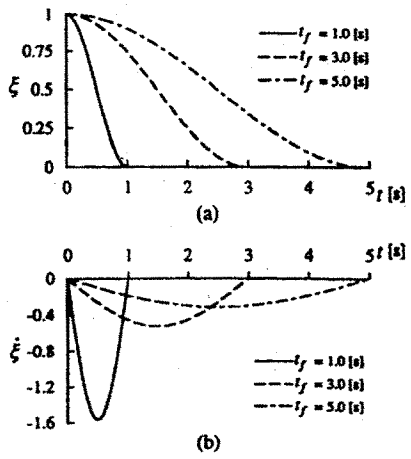

Fig. 1: Time history of ξ and $\dot{\xi}$ for the different prespecified time

3.1 Virtual time ν and TBG

The relationship between actual time t and virtual time ν is given by

$$\frac{d\nu}{dt} = a(t)\,, \tag{6}$$

where the continuous function $a(t)$, called the time scale function [7], is defined as follows:

$$a(t) = -p\frac{\dot{\xi}}{\xi}\,, \tag{7}$$

where p is a positive constant and $\xi(t)$ is a non-increasing function called the Time Base Generator (TBG) [5] [6] generates a bell-shaped velocity profile satisfying $\xi(0) = 1$ and $\xi(t_f) = 0$ with the convergence time t_f. The dynamics of ξ is defined as follows:

$$\dot{\xi} = -\gamma(\xi(1-\xi))^\beta, \tag{8}$$

where γ is a positive constant that can control the convergence time t_f, and β is also a positive constant, $0 < \beta < 1.0$, which determines the behavior of ξ. The convergence time t_f can be calculated with the gamma function $\Gamma(\,\cdot\,)$ as

$$t_f = \int_0^{t_f} dt = \int_1^0 \frac{d\xi}{\dot{\xi}} = \frac{\Gamma^2(1-\beta)}{\gamma\Gamma(2-2\beta)}. \tag{9}$$

Thus, the system converges to the equilibrium point $\xi = 0$ in the finite time t_f if the parameter γ is chosen as

$$\gamma = \frac{\Gamma^2(1-\beta)}{t_f\Gamma(2-2\beta)}. \tag{10}$$

Figure 2 show the time histories of ξ and $\dot{\xi}$ depending on convergence time $t_f = 1.0, 3.0, 5.0$ [s] under the parameter $\beta = 0.5$.

From (6) and (7), the virtual time ν can be represented with respect to ξ as follows:

$$\nu = \int_0^t a(t)\, dt = -p \ln \xi(t) \,. \tag{11}$$

It is obvious that the virtual time ν given in (11) never goes backward against the actual time t. We take this virtual time ν as a new time scale in time scale transformation of the original system (1).

3.2 Time Scaling of the System

The system given in (1) can be rewritten in the virtual time scale as

$$\frac{d}{d\nu} \boldsymbol{X} = \frac{d\boldsymbol{X}}{dt}\frac{dt}{d\nu} = \frac{1}{a(t)} \dot{\boldsymbol{X}} \,. \tag{12}$$

Also, if we apply the state and input transformation with the new state variable $\boldsymbol{\Psi}$ and the new input $\boldsymbol{F_\Psi}$ defined as

$$\boldsymbol{\Psi} = (\Psi_1, \Psi_2, \cdots, \Psi_{2n})^T = (\boldsymbol{x}^T, \frac{\dot{\boldsymbol{x}}^T}{a(t)})^T \,, \tag{13}$$

$$\boldsymbol{F_\Psi} = \frac{d}{d\nu}\left(\frac{1}{a(t)}\right)\dot{\boldsymbol{x}} + \frac{1}{a^2(t)} \boldsymbol{F_X} \,, \tag{14}$$

to the system (12), the new linear system in the transformed time scale is obtained as follows:

$$\frac{d}{d\nu}\boldsymbol{\Psi} = \boldsymbol{P\Psi} + \boldsymbol{Q F_\Psi} \,. \tag{15}$$

As previously defined in the relation between actual time and virtual time, stability of the new system given in (15) is the same as the original system (1) in the actual time [7]. Hence, there exists a feedback control law to stabilize the new system (15) asymptotically.

3.3 Design of the feedback control law

In this subsection, we design the feedback control law with the APFA to stabilize the new system given in (15) in the virtual time scale. Here, we can define the potential function with quadratic form V_Ψ for the new system (15) as follows:

$$V_\Psi = \frac{1}{2} \boldsymbol{\Psi}^T \boldsymbol{K}_0 \, \boldsymbol{\Psi} \,. \tag{16}$$

If we define the feedback control law $\boldsymbol{F_\Psi}$ based on V_Ψ as

$$\boldsymbol{F_\Psi} = -\boldsymbol{K}_1 \, \boldsymbol{\Psi} \,, \tag{17}$$

the time-derivative of the potential function in the new time scale yields

$$\frac{d}{d\nu} V_\Psi = -\boldsymbol{\Psi}^T \boldsymbol{K}_2 \, \boldsymbol{\Psi} \leq 0 \,. \tag{18}$$

The new system is stabilized asymptotically by means of the designed feedback controller $\boldsymbol{F_\Psi}$ in the virtual time scale.

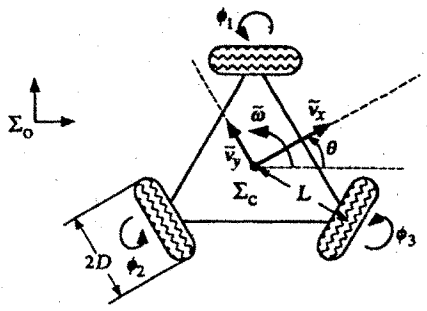

Fig. 2: Omnidirectional mobile robot

By inverse transformation of the time scale from virtual time ν to actual time t for the derived stabilizer $\boldsymbol{F_\Psi}$ with (13) and (14), we can obtain the following feedback control law $\boldsymbol{F_X}$ for the original system (1) as:

$$\boldsymbol{F_X} = -a^2(t) \boldsymbol{K}_3 \, \boldsymbol{x} + \left(-a(t) + \frac{\dot{a}(t)}{a(t)}\right) \dot{\boldsymbol{x}} \,. \tag{19}$$

Now, infinite time in the virtual time scale is corresponding to a finite time t_f in the actual time scale. Therefore, the previous inverse time scale transformation for the feedback controller $\boldsymbol{F_\Psi}$ can be considered as the compression of the virtual time scale. This implies that the state variable $\boldsymbol{\Psi}$ is converged to zero by the feedback control law $\boldsymbol{F_X}$ given in (19) at the specified time t_f.

4 Trajectory generation of an omnidirectional mobile robot

In this section, we apply the proposed method to the trajectory generation of an omnidirectional mobile robot as an example and show its effectiveness from some computer simulations.

4.1 Feedback controller for the vehicle

Figure 2 shows the omnidirectional mobile robot [9] which has three omnidirectional wheels located at the vertices of a cart that has the form of an equilateral triangle enabling it to move omnidirectionally without any reorientation at each time instant. In the figure, Σ_o denotes the world coordinate system with its origin set at the target point for the vehicle and Σ_c denotes the moving coordinate system fixed to the vehicle with its origin set at the center of the cart. The x_c axis is oriented as the direction of motion of the vehicle. Thus, we can choose the following generalized coordinates of the vehicle: position (x, y) and orientation angle θ of Σ_c with respect to Σ_o.

We denote the translational velocity in the x, y direction and the rotational velocity of the robot, respectively, as $\tilde{v}_x$, $\tilde{v}_y$ and $\tilde{\omega}$, and the angular velocity of each wheel as $\dot{\phi}_1, \dot{\phi}_2, \dot{\phi}_3$. The relationship between the driving velocity vector $\boldsymbol{v}_c = (\tilde{v}_x, \tilde{v}_y, \tilde{\omega})^T$ and the

wheel velocity vector $\dot{\phi} = (\dot{\phi}_1, \dot{\phi}_2, \dot{\phi}_3)^T$ is given by

$$\boldsymbol{v}_c = -D \begin{pmatrix} -\frac{1}{\sqrt{3}} & 0 & \frac{1}{\sqrt{3}} \\ \frac{1}{3} & -\frac{2}{3} & \frac{1}{3} \\ \frac{1}{3L} & \frac{1}{3L} & \frac{1}{3L} \end{pmatrix} \dot{\boldsymbol{\phi}}, \qquad (20)$$

where D is the radius of the wheel and L is the distance between the center of the vehicle and wheels, respectively (see Fig. 2). The kinematic relationship between two velocity vectors represented in Σ_o and Σ_c under the rolling-without-slipping condition is given by

$$\dot{\boldsymbol{x}} = \boldsymbol{R}^T \boldsymbol{v}_c, \qquad (21)$$

where $\dot{\boldsymbol{x}}$ denotes the time-derivative of the generalized coordinate vector $\boldsymbol{x} = (x, y, \theta)^T$ and $\boldsymbol{R}$ denotes the rotational matrix with respect to θ as

$$\boldsymbol{R} = \begin{pmatrix} \cos\theta & \sin\theta & 0 \\ -\sin\theta & \cos\theta & 0 \\ 0 & 0 & 1 \end{pmatrix}.$$

The dynamic model under the assumption that no friction exists along the axle is given with the generalized force F_x, F_y and τ by

$$\boldsymbol{M}_o \left(\ddot{\boldsymbol{x}} - \dot{\boldsymbol{R}}^T \boldsymbol{R} \dot{\boldsymbol{x}} \right) = \boldsymbol{F}_o, \qquad (22)$$

where $\boldsymbol{F}_o = (F_x, F_y, \tau)^T$, $\boldsymbol{M}_o = \mathrm{diag.}(m_r + \frac{3I_w}{2D^2}, m_r + \frac{3I_w}{2D^2}, I_r + \frac{3I_w L^2}{D^2})$, m_r is the mass of the vehicle, I_r is the moment of inertia of the vehicle around the center of the cart and I_w is the moment of inertia of the wheel around the axle.

Then, we can rewrite the dynamic equation given in (22) as the following linear system:

$$\frac{d}{dt}\boldsymbol{X} = \begin{pmatrix} \boldsymbol{0}_{3\times3} & \boldsymbol{I}_{3\times3} \\ \boldsymbol{0}_{3\times3} & \boldsymbol{0}_{3\times3} \end{pmatrix} \boldsymbol{X} + \begin{pmatrix} \boldsymbol{0}_{3\times3} \\ \boldsymbol{I}_{3\times3} \end{pmatrix} \boldsymbol{F}_X, \qquad (23)$$

where the state variable vector $\boldsymbol{X} = (\boldsymbol{x}^T, \dot{\boldsymbol{x}}^T)^T \in \Re^6$, and the input vector $\boldsymbol{F}_X = \boldsymbol{M}_o^{-1}\boldsymbol{F}_o + \boldsymbol{R}^T \dot{\boldsymbol{R}} \dot{\boldsymbol{x}}$. Thus, applying the results of **3.3**, we can readily obtain the following state feedback control law $\boldsymbol{F}_X$ for the vehicle:

$$\boldsymbol{F}_X = -a^2(t)\boldsymbol{K}_X \boldsymbol{x} + \left(-a(t) + \frac{\dot{a}(t)}{a(t)} \right) \dot{\boldsymbol{x}}, \qquad (24)$$

with the gain matrix $\boldsymbol{K}_X = \mathrm{diag.}(\frac{k_1}{k_4}, \frac{k_2}{k_5}, \frac{k_3}{k_6})$ under $k_i > 0$ $(i = 1, 2, \cdots, 6)$.

In the next subsection, the analysis on the dynamic behavior of the state variable $\boldsymbol{X}$ of the system (23) is discussed.

4.2 Convergence of the state variable X

Substituting the feedback control law $\boldsymbol{F}_X$ given in (24) into the original linear system equation given in (23), we have the second-order differential equation as follows:

$$\ddot{\boldsymbol{x}} = -p^2 \left(\frac{\dot{\xi}}{\xi} \right)^2 \boldsymbol{K}_X \boldsymbol{x} + \left\{ (p-1) \left(\frac{\dot{\xi}}{\xi} \right) + \left(\frac{\ddot{\xi}}{\dot{\xi}} \right) \right\} \dot{\boldsymbol{x}}. \qquad (25)$$

Here, we first analyze the behavior of the vehicle on the x coordinate. From (25), the following Euler's equation with respect to x and ξ can be derived:

$$\xi^2 \frac{d^2x}{d\xi^2} - (p-1)\,\xi \frac{dx}{d\xi} + \frac{k_1}{k_4} p^2 x = 0. \qquad (26)$$

Solving the above non-linear differential equation for x, the dynamic behavior in the x coordinate of the vehicle is represented according to the discriminant of the characteristic polynomial of (26), $D_x = 4\frac{k_1}{k_4} - 1$, as follows:

(A) if $D_x > 0$

$$x = x_0 \left\{ \cos\left(\frac{\sqrt{D_x}}{2} p \ln\xi \right) - \frac{1}{\sqrt{D_x}} \sin\left(\frac{\sqrt{D_x}}{2} p \ln\xi \right) \right\} \xi^{\frac{p}{2}}. \qquad (27)$$

(B) if $D_x = 0$

$$x = x_0 \left(1 - \frac{p}{2} \ln\xi \right) \xi^{\frac{p}{2}}. \qquad (28)$$

(C) if $D_x < 0$

$$x = \frac{x_0}{\lambda_2 - \lambda_1} \left(\lambda_2 \xi^{\lambda_1} - \lambda_1 \xi^{\lambda_2} \right), \qquad (29)$$

$$\lambda_1 = \frac{p}{2} + \frac{\sqrt{-D_x}}{2} p, \quad \lambda_2 = \frac{p}{2} - \frac{\sqrt{-D_x}}{2} p,$$

where x_0 is the initial position of the vehicle in x coordinate. Since the non-increasing function ξ converges to zero at finite time t_f, the necessary and sufficient condition to converge x, $\dot{x}$ and $\ddot{x}$ to zero at the specified time t_f is given as follows depending on the discriminant D_x :

$$(1)\, if \;\; D_x \geq 0 \;\; then \;\; p > 4(1-\beta),$$
$$(2)\, if \;\; D_x < 0 \;\; then \;\; p > \frac{4(1-\beta)}{1-\sqrt{-D_x}}.$$

The dynamic behavior of the other state variables y and θ can be analyzed in the same manner. It can be concluded that the feedback control law $\boldsymbol{F}_X$ (24) designed using the proposed method can regulate the dynamic behavior of the mobile robot and the convergence time to reach the goal.

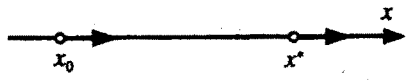

Fig. 3: Generation of a straight trajectory

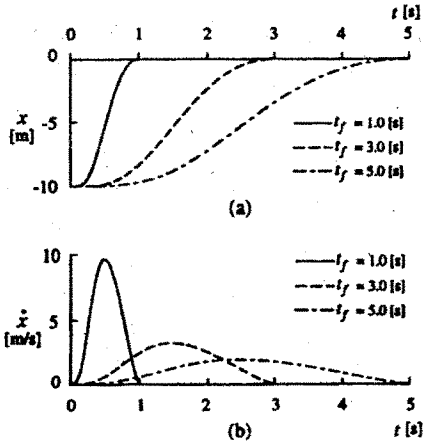

Fig. 4: Time histories of position and velocity for the different prespecified time generated by the proposed method ($D_x < 0$)

4.3 Computer simulations

4.3.1 Generation of straight trajectories

In 4.2, it is proven that the dynamic behavior of the vehicle is completely dominated by ξ. First of all, let us consider the case of $x_0 = (x_0, 0, 0)^T$, i.e., the initial position is on the x axis and the initial orientation is $\theta_0 = 0$[rad] as shown in Fig. 3. Therefore, the y coordinate and the orientation θ of generated trajectory will always be zero.

Figure 4 shows the time histories of x, $\dot{x}$ and $\ddot{x}$ generated by the proposed method for the initial position of the vehicle ($x_0 = (-10$ [m], 0 [m], 0 [rad]$)^T$) depending on three different convergence times $t_f = 1.0$, 3.0, 5.0 [s] under the parameters $k_1/k_4 = 0.125$ [s^{-1}], $\beta = 0.5$, $p = 8.0$. In this case, the discriminant D_x is less than zero, i.e., the dynamic behavior is dominated by (29), thus generating an overdamped trajectory. It can be verified from Fig. 4 that the vehicle generates smooth trajectories and reaches the target position at the specified time t_f. This observation indicates that the proposed method can naturally generate a straight path for the vehicle with an easily controllable transient response via the parameters of the TBG.

Figure 5 shows the time histories of the potential function V_X and V_Ψ. In Fig. 5(a), we can see that V_X converges to zero at the designated time t_f but not monotonically. On the other hand, V_Ψ is non-increasing and converges to zero as shown in Fig. 5(b), since the feedback controller is designed for the state variable Ψ in virtual time scale. It should be noticed from Fig. 4 that the time histories of the potential function depicted in Fig. 5 converges to zero at the designated time t_f in all cases.

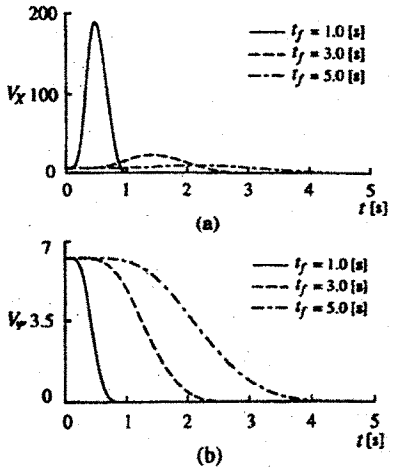

Fig. 5: Time histories of potential function V_X and V_Ψ for the different prespecified time

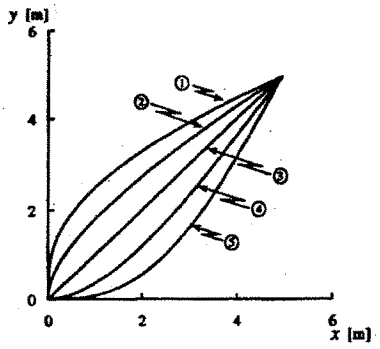

Fig. 6: Change of the generated trajectories with the different sets of the feedback gains, k_1/k_4 and k_2/k_5 ($D_i \leq 0 : i = x, y$)

Table 1: Feedback control gains used in the simulation

Set of Gains	①	②	③	④	⑤
k_1/k_4 [s^{-1}]	0.25	0.25	0.25	0.175	0.125
k_2/k_5 [s^{-1}]	0.125	0.175	0.25	0.25	0.25

4.3.2 Generation of curved trajectories

Figure 6 shows the change of the generated trajectories from the initial position $x_0 = (\frac{7}{\sqrt{2}}$ [m], $\frac{7}{\sqrt{2}}$ [m], 0 [rad]$)^T$ to the goal set at the origin of the world coordinate Σ_o with the different sets of feedback gains: k_1/k_4 for the x direction and k_2/k_5 for the y direction as shown in Table 1. All sets satisfy the condition that $D_i \leq 0$ ($i = x, y$) under the parameters $\beta = 0.5$, $p = 8.0$ and $t_f = 5.0$ [s]. It is verified that the proposed method can generate various trajectories by changing the feedback gains.

The change of the time histories of the generated trajectories and the potential function V_X and V_Ψ is

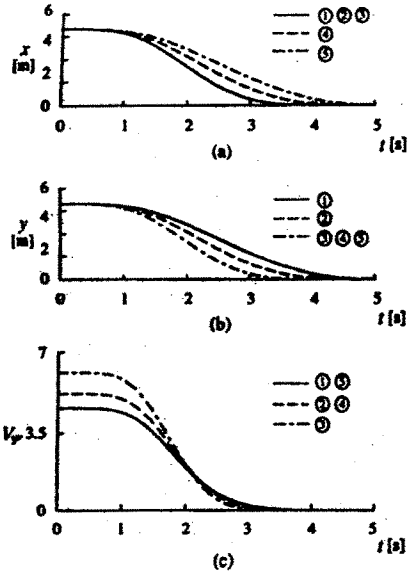

Fig. 7: The generated temporal trajectories and time histories of potential function V_ψ for the different sets of the feedback gains, k_1/k_4 and k_2/k_5

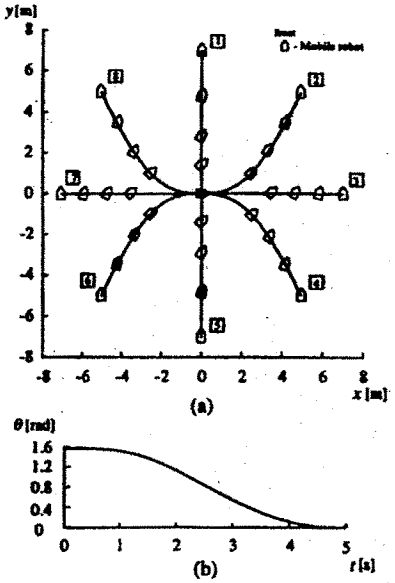

Fig. 8: Trajectories for 8 initial states generated by the proposed method ($D_i \leq 0 : \ i = x, y, \theta$)

shown in Fig. 7. The vehicle reached the target position at the convergence time $t_f = 5.0$ [s].

Figure 8 shows the simulation results generated by the proposed method for several initial positions located at different points on the circle with a radius of 7[m] and the initial orientation $\frac{\pi}{2}$ [rad] under the parameters $k_1/k_4 = 0.125$ [s^{-1}], $k_2/k_5 = 0.25$ [s^{-1}], $k_3/k_6 = 0.125$ [s^{-1}], $\beta = 0.5$, $p = 8.0$ and $t_f = 5.0$ [s]. The vehicle reached the goal via generation of smooth trajectories for all initial positions.

5 Conclusions

In this paper, the new trajectory generation method for the dynamic model of robots using the concept of the APFA and the time scaling transformation has been presented. In simulation results with the omnidirectional mobile robot, the effectiveness of the proposed method was ascertained. Since the proposed method can specify the necessary time that the robots reach the goal, it may be useful for time scheduling problems of a robot or the synchronous control of multiple robots.

References

[1] O. Khatib, "Real-time obstacle avoidance for manipulators and mobile robots," International Journal of Robotics Research, Vol. 5, No. 1, pp. 90–98, 1986.

[2] J. O. Kim and K. Khosla, "Real-time obstacle avoidance using harmonic potential functions," IEEE Trans. on Robotics and Automation, Vol. 8, No. 3, pp. 338–349, 1992.

[3] S. Sundar and Z. Shiller, "Optimal obstacle avoidance based on the Hamilton-Jacobi-Bellman equation," IEEE Trans. on Robotics and Automation, Vol. 13, No. 2, pp. 305–310, 1997.

[4] H. Hashimoto, Y. Kunii, H. Harashima, V. I. Utkin, S. A. Krasnova, and I. M. Kaliko, "Sliding mode control and potential fields in obstacle avoidance," in Proceedings of European Control Conference, pp. 859–862, 1993.

[5] T. Tsuji, P. Morasso and M. Kaneko, "Feedback control of nonholonomic mobile robots using time base generator," in Proceedings of IEEE International Conference on Robotics and Automation, pp. 1385–1390, 1995.

[6] T. Tsuji, K. Chigusa and M. Kaneko, "Trajectory generation of moving robots using active deformation of artificial potential fields," Journal of Japan Society of Mechanical Engineers, Vol. 62, No. 597, pp. 1905–1911, 1996, In Japanese.

[7] M. Sampei and K. Furuta, "On time scaling for nonlinear systems: Application to linearization," IEEE transactions on Automatic Control, Vol. 31, No. 5, pp. 459–462,1986.

[8] M. Sampei, T. Tamura and T. Itoh, "Path tracking control of a trailer-like mobile robot," in Proceedings of IEEE/RSJ, International Workshop on Intelligent Robots and Systems'91, pp. 193–198, 1991.

[9] C. Canudas de Wit, B. Siciliano and G. Bastin (Eds), "Theory of robot control," Springer, pp. 277–278, 1996.